Joint shear behaviour revised on the basis of morphology 3D modelling and shear displacement

Guy Archambault, Rock Flamand, Sylvie Gentier, Joëlle Riss, Colette Sirieix

PROCEEDINGS OF THE 2ND NORTH AMERICAN ROCK MECHANICS SYMPOSIUM: NARMS'96
A REGIONAL CONFERENCE OF ISRM/MONTRÉAL/QUÉBEC/CANADA/19-21 JUNE 1996

Rock Mechanics Tools and Techniques

Edited by
MICHEL AUBERTIN
Ecole Polytechnique, Montréal, Québec, Canada
FERRI HASSANI
McGill University, Montréal, Québec, Canada
HANI MITRI
McGill University, Montréal, Québec, Canada

OFFPRINT

A.A. BALKEMA/ROTTERDAM/BROOKFIELD/1996

Rock Mechanics, Aubertin, Hassani & Mitri (eds) © 1996 Balkema, Rotterdam. ISBN 90 5410 838 X

Joint shear behaviour revised on the basis of morphology 3D modelling and shear displacement

Guy Archambault & Rock Flamand – *Centre d'Études sur les Ressources Minérales, Université du Québec à Chicoutimi, Qué., Canada*

Sylvie Gentier – *BRGM, Direction de la Recherche, Orléans, France*

Joelle Riss – *Centre de Développement des Géosciences Appliquées, Université de Bordeaux I, Talence, France*

Colette Sirieix – *ANTEA, Direction de la Géotechnique, Orléans, France*

ABSTRACT: Joint shear behavior is rediscussed on the basis of a 2D statistical characterization and a 3D modelling of a joint roughness morphology. The shear processes and progressive degradation phenomena on the joint surfaces are analyzed in relation with normal stress and shear displacement. These discussion and analysis are based on the results of an experimental study on the shear behavior of unfilled natural rock joint replicas.

1 INTRODUCTION

The behavior of single, irregular joints submitted to direct shear conditions, under either constant normal stress or constant normal stiffness, is very complex. Scholtz (1990) stated that there is no constitutive law for friction quantitatively built upon micro-mechanical framework because of the complexity of shear contacts, the topography of contacting surfaces and the evolving surfaces topography during sliding. Even if a numberless research works were done in the last three decades, to solve various problems in relation with joint shear behavior, on which the ISRM Commission on Rock Joints organized three symposium (Stephansson 1985; Barton & Stephansson 1990; Goodman & Myer 1992), a recent review of the literature (Stephansson & Jinq 1995) pointed out that there is still a large number of problems to solve before an overall understanding of the phenomenon. Over this period, a large number of models were formulated to predict rock joint shear strength (Patton 1966; Ladanyi & Archambault 1969; Barton 1973; Swan & Zonggi 1985; Haberfield & Johnston 1994; to cite a few), several of which were compared on the basis of appropriate physical constraints for empirical relations and their ability to satisfy the principles of mechanics (Gerrard 1986). Other models were proposed for the deformability of rock joints (Goodman 1976; Bandis et al. 1981; Gentier 1986; Saeb & Amadei 1992). While these models of joints have substantially improved our understanding of rock joint behavior, their limitations must also been recognized.

The mechanical properties of rock joints depend essentially on the degree of matching between the joint walls; on the surface of contact between them; on their morphological characteristics; on the magnitude of normal stress (or load) acting on them as well as the rock material properties of the joint walls and the presence of infilling materials. The dominant factor, influencing practically all these aspects of the mechanical behavior or rock joints, is the roughness morphology and the difficulty is its characterization and modelling (Stephansson & Jing 1995).

Joint roughness profiles provide an incomplete and biased characterization of the surface morphology (Riss & Gentier 1990). Very few works account for joint walls asperity angularity distribution in modelling the mechanics of rock joint shear behavior and particularly none has done an attempt to integrate a 3D representation of the surfaces morphology. Few works have been dedicated to the progressive degradation of the joint surface asperities with shear displacement (except for cyclic shear) and normal stress. Regarding the geometrical description of joint surfaces morphology, an approach is proposed on the basis of a 3D statistical modelling. Up to the present, studies on prediction of rock joint behavior under shear conditions were mainly limited to apply 2D statistical parameters to empirical model of joint shear strength with more or less success.

These observations and the basic concepts for modelling joint shear process on irregular surfaces are discussed on the basis of 3D statistical description of joint surfaces morphology in relation with direct shear test results from natural joint replicas submitted to constant normal stress loading conditions for given shear displacements.

2 CHARACTERIZATION OF JOINT SURFACES ROUGHNESS AND 3D MODELLING

The 3D geometry of asperities on the joint wall surfaces affects both the stress distribution and the zones of degradation on them, during shear displacement. Knowing the joint wall surfaces morphology, means here that a 3D quantitative description of their initial

state and their evolution is done during direct shear tests. To do so, a series of identical replicas from the walls of a natural fracture sample, drilled perpendicular to the fracture plane, in the Gueret Granite (France), were realized. The characterization of this fracture surface morphology has been studied in detail (Gentier 1986; Riss & Gentier 1989, 1990) while the replicas preparation and cement mortar characteristics may be found in Flamand et al. (1994). These replicas were submitted to direct shear tests under three different normal stress and each shear test was stopped at defined shear displacement for five (5) displacements. This procedure permits a good control on the evolution of the joint wall surfaces morphology.

At the end of each shear test (the shear stress, shear displacement, normal stress and normal displacement being available), a morphological analysis was performed using profiles z = f(x,y) recorded on the joint wall surfaces by means of a laboratory profilometer developed by the BRGM research division. The profiles were recorded at the same positions on each wall surfaces of the fracture replica and kept constant from one shear test to the other and this for each normal stress and shear displacement tested, following a prescribed procedure (Flamand et al. 1994), so that they can be compared on a qualitative and quantitative basis. This procedure permits, for the first time, simultaneous recording in an overall data set the mechanical shear test results and surface characteristics of the morphology evolution for various normal stress and shear displacements. The analysis of these data consists in the deduction of parameters characterizing the whole set of recorded points i.e. the joint wall surface expanding in a 3D space, and in detailed distribution analysis of the θ_2 angles, between a reference plane and a line segment linking two successive points on the recorded profiles. This analysis is fundamental to restore the 3D colatitude θ_3 distribution of elementary plane facets composing the joint wall surfaces before and after testing (Riss et al. 1995). Geometric definitions of 2D angularity θ_2 on profiles and 3D angularity θ_3 on facets in 3D space are shown in Fig. 1A, while Fig. 1B illustrates the bias introduced by the profiles on 2D angularity θ_2 when they do not pass by the peak of asperities, situation that has a low probability to occur in systematic profiling. This may be corrected in choosing profiles through peaks (a difficult task) or restoring 3D colatitude θ_3 distribution of the elementary plane facets.

The overall analysis of the joint wall surfaces gives a global view of their morphology and depends on whether we are interested in the 3D spatial reality of each joint wall surface or to each joint wall surface recording directions related respectively to:

a) the total variance of all profiles set of points, the residual variance and correlation coefficient after linear regression of the altitudes z in function of the coordinates (x,y) on the reference plane, the azimuth and colatitude in a given reference system of the regression plane and of the principal plane resulting from the diagonalization of variance and covariance matrices of the whole set of points; or

b) the linear roughness coefficients (R_L, the z_2, z_3 and z_4 and the linear regression parameters ($\theta_{regression}$ and residual variance $S^2_{z,x}$).

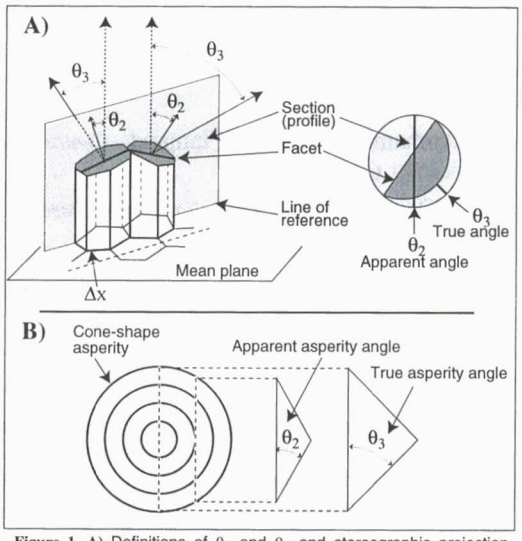

Figure 1. **A)** Definitions of θ_2 and θ_3 and stereographic projection showing the dependance of θ_2 on θ_3 the direction of the vertical section plane (From Riss & Gentier, 1989). **B)** Illustration of the bias 2d apparent asperity angle θ_2 relatively to the true asperity angle given by θ_3.

The analysis performed on the joint wall surfaces under study permits to establish that the local mean plane dips slightly (5°) in a direction perpendicular to the shear direction, the upper wall dips slightly more than the lower one and the lower wall is rougher than the upper one; while the computation of the linear roughness coefficients measured on profiles parallel to the shear direction are tabulated in Table 1. The details of these analyses and computations appear in Riss et al. (1995) and profiles are illustrated in Fig. 2.

The detailed analysis is based on the colatitudes distributions evaluation. On a descriptive point of view, histograms and classic characteristics of angular distributions (mean, variance,...) are computed and the obtained distributions after each test are compared to the distribution before testing (the Chi-square test). Inference permits to estimate the colatitudes θ_3 distribution and a theoretical model is adjusted on it. The colatitudes θ_3 distribution modelling is a necessary prerequisite condition to compute the parameters characterizing the surface roughness before and after shear testing. These parameters are the surface roughness coefficient R_A and the position (directional mean) and dispersion (variance) characteristics of the distribution $F(\theta_3)$. All this is easily done through a

Table 1. Classical linear roughness coefficients measured on profiles parallel to the shear direction.

Profile	R_L		z_2		z_3		$\theta_{regression}$ z=f(x)		$S^2_{z,x}$ mm2		z_4	
	A	B	A	B	A	B	A	B	A	B	A	B
1	1.029	1.029	0.251	0.246	0.547	0.608	1°59	1°63	0.108	0.092	0.089	0.190
2	1.030	1.031	0.249	0.254	0.528	0.551	0°56	0°64	0.281	0.286	0.111	0.220
3	1.033	1.033	0.263	0.264	0.597	0.581	-0°74	-0°76	0.327	0.321	-0.018	0.024
4	1.041	1.036	0.300	0.283	0.611	0.521	0°05	0°02	0.585	0.552	0.057	0.101
5	1.022	1.030	0.212	0.254	0.448	0.561	-1°88	-1°68	0.702	0.637	-0.017	0.048
6	1.042	1.043	0.300	0.306	0.556	0.590	-0°34	-0°37	0.493	0.485	0.136	0.103

statistical PC computer programs package developed for these purposes (Riss et al. 1995).

Figures 3 and 4 summarize this detailed analysis for the joint wall surfaces studied with the computed linear roughness coefficients (Table 1), dependent on θ_2 distributions, from which several observations, important for the joint shear behavior, can be drawn. Figure 3 indicates on the basis of the 2D colatitudes distributions characteristics, that the probabilities for positive θ_2 is a bit higher than for the negative θ_2, but the mean values of the later are smaller than the other one. In average there are more aspirities in the positive direction than in the opposite one but the asperities are smoother at the recording scale. On the whole repartitions of positive and negative angles can be considered as identical for wall A and slightly more dispersed for wall B. Also, from Table 1, the parameters $\theta_{regression}$ and $S^2_{z,x}$ indicate the trend of the profiles to dip and the later measures the part of the elevations z that are not explained by the global dip of the fracture replica. This is illustrated in Fig. 2 in which the dipping trend of profiles 1, 4 and 5 are shown and can indicate probable zones where asperities may be damaged, particularly for those on profiles dipping towards the shear direction. But the probability of damaging depends also on asperities heights (CLA, RMS,...), profiles roughness (R_L), roughness dispersion ($S^2_{z,x}$) and the other roughness coefficients. So, looking at one of them without taking into account informations from the others can introduce large errors and biased informations on the morphology of the surfaces. Moreover, 2D roughness parameters are insufficient to describe adequately the joint wall surfaces morphology changing from point to point as well as the stress distribution on them.

Digitized profiles looks like polygonal lines and, in the same manner, a polygonal surface of a joint wall results from its intersection with a set of contiguous hexagonal prisms orthogonal to the mean regional plane. Then the surface is subdivided into small facets, small enough to be considered to be planar (Fig. 1A). Angles between the normal to the facets and z axis are called true colatitudes (θ_3). As

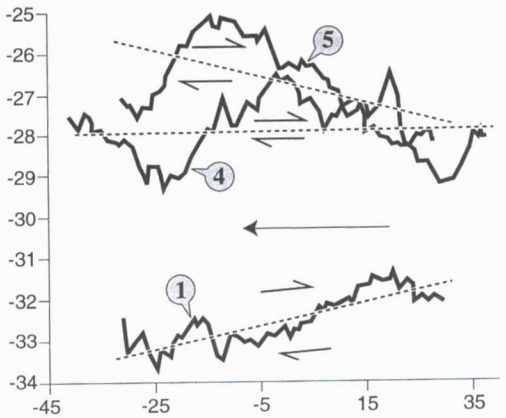

Figure 2. Profiles No 1, 4, and 5 of the lower wall (direction 0°) with their local regression lines in the vertical plane in which σn and shear direction (arrow) are located. Units on the axis are mm.

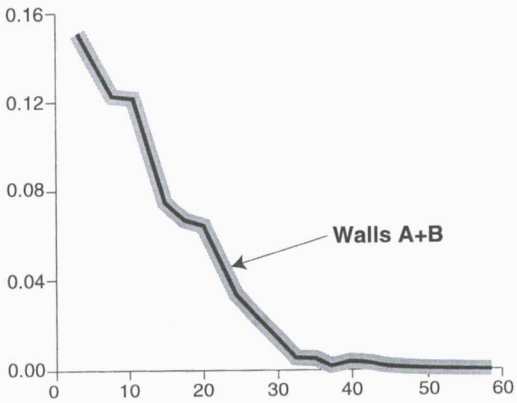

	$P(\Theta_2 > 0)$	$P(\Theta_2 <= 0)$	$\overline{\Theta}_2 +$	$\overline{\Theta}_2 -$
Wall A	**0.53**	**0.47**	**10°31**	**-11°91**
Wall B	**0.56**	**0.44**	**10°08**	**-12°49**

Figure 3. Relative frequencies of experimental 2D colatitudes θ2 for gathered positive and negative θ2 with some charateristics of the colatitudes distributions.

shear direction is parallel to the local mean plane horizontal direction, it is assumed that 2D colatitudes, measured in vertical planes in this direction, can represent any colatitude measured in a plane perpendicular to the local mean plane. Using classical method of 3D colatitude reconstruction (Gentier 1986), inference of the experimental 3D colatitudes distributions is done (Fig. 4). As the 2D distributions are not strictly similar, so are the reconstructed distributions. With these distributions, areal roughness (R_A) can be computed in order to evaluate, by comparison, the reconstructed distributions $F(\theta_3)$ using R_A values derived with a stereological method. The $F(\theta_3)$ distributions being acceptable then theoretical models must be fit to them in order to have an expression, useful for further developments such as a simulation of the fracture wall surfaces and for estimating R_A. Theoretical distributions are inferred either by fitting the 3D empirical distribution derived from the 2D (θ_2) distribution to a model or by fitting the 2D experimental (θ_2) to a 2D distribution from a 3D model (Riss & Gentier 1989 and 1990). The 3D models used are generalized axial distributions:

$$F(\theta_3) = \frac{\text{Exp}\,(K\cos\beta)}{\int_0^1 \text{Exp}(Kt\beta)dt} \sin\Theta_3$$

Models derived from fitting are shown in Fig. 4 with the parameters used and the characteristics deduced for R_A, the mode and the mean ($\bar{\theta}_3$).

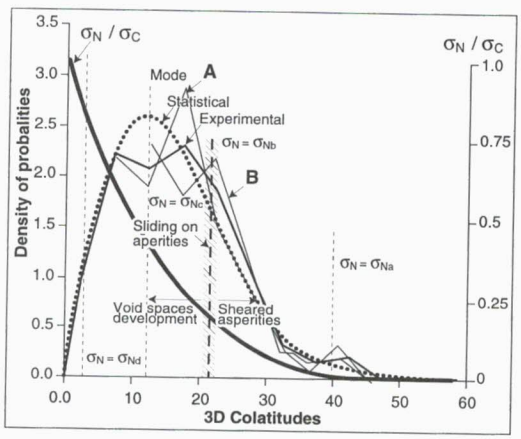

	K	β	R_A	Mode	$\bar{\theta}_3$
Wall A	16.58	1.10	1.0634	13°	16°11
Wall B	15.08	1.25	1.0625	13°	15°96
A + B	12.06	1.65	1.0632	13°	15°88

Figure 4. 3D reconstructed distributions and models for colatitudes θ_3 with characteristics of the fitted models for 3D distribution.

They are quite close one from the other, but the most important result is that the 3D elementary facets dip in any direction with a mean angle of 16° and this angle is obviously greater than the 2D mean angle of individual segments (Riss et al. 1995).

The previous global and detailed analyses permit to establish that a perfect matching of the joint wall surfaces is highly improbable with the differential variation between walls dipping and roughness as well as between 2D colatitudes (θ_2) distributions of asperities on both walls. Moreover, Gentier (1986) in its evaluation of voids between the joint walls has illustrated a series of profiles of both walls adjusted together which show large void spaces and few contact areas between them. The same was illustrated by Flamand et al. (1994) for a single profile of the joint replicas under study. Most of the contacts are located on the slopes of asperities and it may happen that on a particular profile no contact can be seen. Of course, the contact areas are varying with applied normal and shear loads on the joint walls and also during shear displacement, so that, it is extremely difficult to evaluate areas of contact between both walls and more with displacements. The only way to do it, is to observe directly the damaged zones at various shear displacement from the pre-peak to the residual post-peak phases. This was the method used and discussed in another paper in this session (Riss et al.).

Anisotropic joint shear behavior in relation with shear direction and sense could be deduced from the previous morphological analyses on the joint wall surfaces. The slight dip (5°) of the tested joint local mean plane perpendicular to the used shear direction, the variations of the profiles with recorded direction, the dissymetry between the positive and negative colatitudes and the variability in attitudes of the profiles in the same direction (backward and forward dipping) are all causes for an anisotropic behavior with direction and sense of shear displacement.

Even with all these quantitative analyses (global probabilities, roughness parameters and coefficients) and the more sophisticated 3D statistical modelling and characterization of joint roughness angularities, giving a more realistic view than the 2D statistical evaluation, no spatial structural information is given for an adequate modelling of shear deformation and strength on joints. Asperities spatial distribution and shapes on joint wall surfaces are not completely at random, the presence of superposed structures (as waviness, jogs and others) can not be detected by the previous analyses. Various methods can be used to do it like spectral, fractal and/or geostatistical analysis; the later being a powerful tool to do this quantitative evaluation of asperities structures. Variograms and variographic analysis of profiles permit to characterize the size of asperities structures (range) while kriging modelling and simulation can restitute the topographic surfaces of the joint (Gentier 1986; Gentier & Riss 1990).

3 JOINT SHEAR BEHAVIOR FROM DIRECT SHEAR TESTS

The direct shear test results were obtained from a shear test program (Flamand et al. 1994) on joint replicas submitted to three different constant normal stress (7, 14 and 21 MPa). The shear tests were performed and stopped, at various shear displacements (0.35, 0.55, 1.0, 2.0 and 5.0 mm) totalizing 15 shear tests. The test results are summarized in Fig. 5.

A detailed analysis of these results was done in Flamand et al. (1994) and Archambault et al. (1995) and can be summarized in the following phases (Fig. 5A):

- phase I: elastic mobilization of shear stress by friction with more or less contractancy (negative dilatancy) on the joint plane and increasing area of contact already observed and called "junction growth" (Tabor 1959);
- phase II: non-linear dilatancy hardening phase mobilization to peak shear stress with increasing dilatancy rate and decreasing area of contact on the joint plane depending on σ_N;
- phase III: peak shear stress (or shear strength) phase, following a behavior between constant peak displacement and constant stiffness models (Goodman 1976) in relation with σ_N, at maximum dilatancy rate with more or less asperities failure and reincreasing contact areas with σ_N;
- phase IV: progressive softening phase (or unstable yielding) with a progressive degradation of the joint surfaces (by asperities micro-fracturing, crushing, ploughing, indentation or failure at the base for high σ_N), decreasing shear stress towards residual strength under a given shear stress gradient (or softening modulus) with decreasing contact normal stresses on the joint in relation with an increasing area of contact, dilatancy still increasing at reduced rate for low to moderate σ_N value;
- phase V: residual strength (or stable sliding) phase in which shear and normal stresses are relatively stable but degradation on the joint surfaces is still operating with shear displacements by friction and wear of asperities as well as grinding of particles

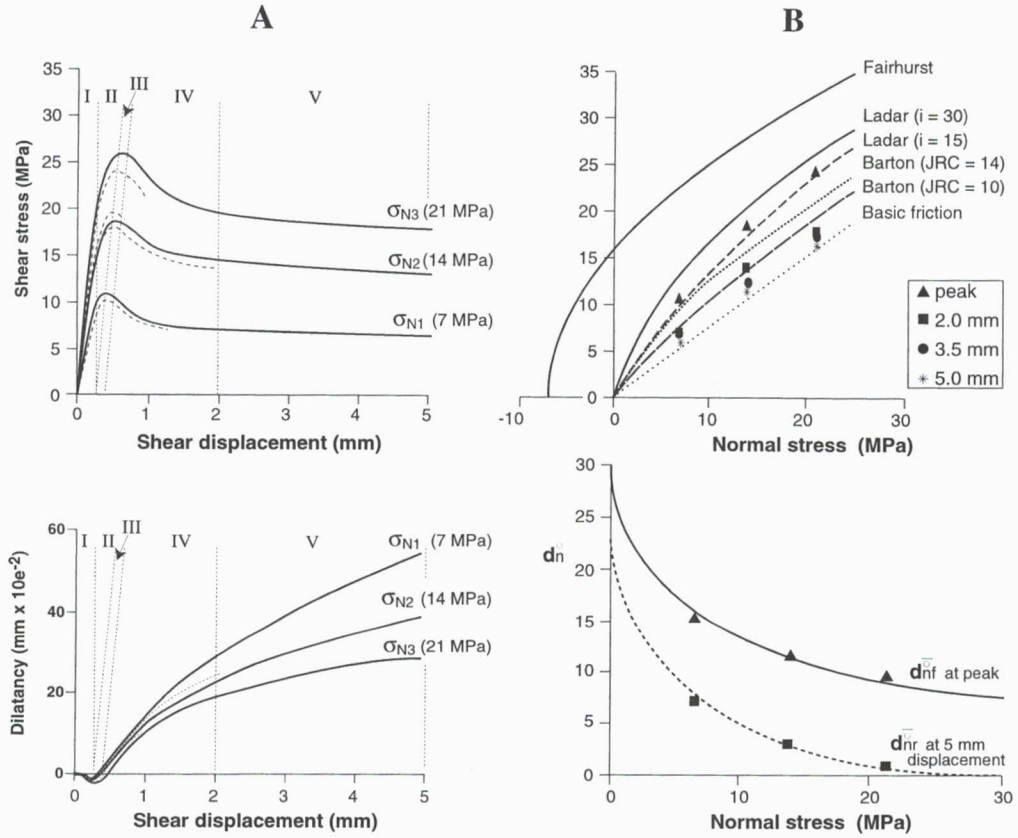

Figure 5. Direct shear test results: **A)** shear stress-displacement-dilatancy relationships and **B)** calculated peak strength envelopes and dilatancy variation with normal stress according to models and test results

to produce gouge material filling valleys and throughs, so that area of contact trends toward mean shear plane area, while dilatancy may still be present but at a very reduced rate (for low to very low σ_N).

The direct shear test results are plotted in a Mohr diagram (upper part, Fig. 5B) while the bottom diagram illustrates the dilatancy rate (or angle) behavior with normal stress (σ_N). These results are compared with LADAR model (Ladanyi & Archambault 1969) for i_0 values of 15° and 30° respectively and with Barton's model (Barton 1973) for JRC values of 10 and 14, limits determined with the z_2 coefficient in Table 1 (Tse & Cruden 1979). A good agreement between experimental results and i_0 values of LADAR model between 15° and 17° corresponding relatively well to the mean $\bar{\theta}_3$ value of 16° (Fig. 4). The same observation regarding dilatancy rate (or angle) behavior with the normal stress where $d\mathring{n}_f$ vary between 14.1° and 10.4° for low σ_N values and this is in better agreement with the reconstructed 3D distribution of asperity angularity discussed in detail in Archambault et al. (1995). A compilation of peak dilation angles and τ/σ_N values from direct shear test results performed on various rock joints by different workers (Barton 1973) including Barton's own results and a lot more in the last decade confirm a certain trend for i_0 values to be between 15° and 35° limits and for $d\mathring{n}_f$ varying between 0° and 25°.

The shear process of a joint with irregular surfaces may be summarized in the following scenario:

i) Application of the normal load concentrates the normal stress on very few points or contact areas with simultaneous closure of the joint depending on normal load magnitude and joint surfaces asperities morphology (Gentier 1986; Bandis et al. 1984). This part is not shown (Fig. 5A).

ii) Shear load gradual application from zero level results in a near closure (negative dilatancy), with an increase of the real contact area until gross slippage is imminent and it may reach three times the initial static area without change in the normal load. However, for any two surfaces, the final area is a numerical constant times the initial area developed without shear forces, so that the proportionality between both forces (shear and normal) at the point of slipping is maintained, and this increase in contact area was described and termed "junction growth" by Tabor (1959). This phase of increasing shear load give rise to a transfer of the stresses on asperities positive slopes defined by their angularity and constitute phase I of linear elastic mobilization of the shear stress in friction on the inclined plane of asperities accompanied by their deformation.

iii) A non-linear shear stress – shear displacement – dilatancy hardening phase follows until peak shear strength is reached, resulting from the mobilization of dilatancy in addition to friction on the facet slopes of asperities involved in areas of contact, with a gradual reduction of contact area and increasing normal stress on it, till failure occurs (phases II and III). Asperities within a restricted domain of angularity, depending on the joint surfaces morphological structures and applied normal stress, in the contact areas are mobilized in friction on the irregular joint plane and control the rate (or angle) of dilatancy in the shear process on the joint plane (Fig. 4). Asperities with higher angularity than the range of those mobilized in friction are deformed and sheared off for very small shear displacement and show frictional behavior thereafter; while asperities with lower angularity are creating voids by separation of the two surfaces of the joints in these areas and the increase in void spaces depends on the dilatancy rate. The selection process of asperities angularity in friction on the distribution is done by the normal stress magnitude, as illustrated alternatively by $\sigma_{Na} < \sigma_{Nb} < \sigma_{Nc} < \sigma_{Nd}$ in Fig. 4, and depends on angularity density of probabilities, on angularity statistical distribution model applied and on asperities structures at different scales.

iv) In the post-peak degradation phases (IV and V) of asperities on the joint surfaces, the contact area is rapidly increased in the unstable phase releasing progressively the concentrated contact normal stresses, towards the joint mean normal stress, with a decreasing shear strength. Finally a large surface of contact in the stable residual strength phase is reached with shear displacement, where degradation is still operating by ploughing, wear and grinding of asperities and particles on the joint shear plane to produce gouge material filling throughs and valleys on it. Dilatancy may still be present at decreasing rate for low σ_N values but will disapear with shear displacement. Like for the other phases, σ_N and asperities morphology on the joint surfaces, and for this phase shear displacement, play a major role.

4 IMPLICATIONS ON ROCK JOINT SHEAR BEHAVIOR AND SRENGTH MODELLING

The previous scenario demonstrates how the normal stress magnitude (σ_N) selects asperities angularity intervening in the simultaneous friction and failure mechanisms on the joint plane during the shear process (Fig. 4). The 3D distribution of colatitudes (θ_3) show for $\theta_3 \geq 30°$ a very low density of asperities having these angularities and their failure will occur at extremely low normal stress. Normal stress as low as $\sigma_N < 0.1\ \sigma_c$ (~ 7 MPa) already show shear strength corresponding to i_0 values near θ_3 mean = 16°, corroborated by dilatancy angle $d\mathring{n}_f$ = 14.1 (Fig. 5B). So, to mobilize θ_3 value (or i_0) beyong the mean ($\theta_3 > 16°$) in friction (without asperities failure) need very low normal stress ($\sigma_N < 0.05\ \sigma_c$) i.e. less than 4 MPa. These low σ_N values are almost the rule in experimental results from direct shear test on joint in the literature and this corresponds to a wide range of stress level observed in the design of workings in jointed rock masses.

Under such conditions, it is difficult to observe all the mechanisms related to rock joints shear behavior. This means that at a given very low normal stress ($\sigma_N < 0.01\ \sigma_c$), i_0 values selected in friction will be around $\theta_3 \geq 30°$, almost no asperities will be sheared off, friction and dilation will be essentially the intervening mechanisms. Shear strength will be given by Patton's model (1966), $\sigma_N = \tan(\phi_b + i)$, or LADAR's model (Ladanyi & Archambault 1969) in which the sheared area ratio as $\cong 0$ and $i = i_0$ corresponding to the θ_3 colatitudes selected. Increasing σ_N to higher values ($\sigma_N > 0.05\ \sigma_c$ to $\sigma_N = 0.3\ \sigma_c$), in which the values tested are, mobilize in friction lower i_0 values near θ_3 mean $\cong 16°$ with normally an increasing proportion of asperities sheared off at peak, usually proportional to $(\sigma_N/\sigma_c)^k$ ratio. Further increments of $\sigma_N > 0.5\ \sigma_c$ must lower to i_0 values mobilized in friction below mean (16°) and mode (13°) progressively with σ_N/σ_c increasing towards 1.0 or transition stress (Fig. 4). This behavior is for asperities distributed at random on the mean joint plane without the presence of major structures such as jogs or steps with high angularity θ_3 not detected in the distribution, then all the shear process will be controlled by these structures even if their colatitude $\theta_3 > 40°$. The limits given by the LADAR model of i_0 value between 15° and 30° are only indicative because the model was developed for regular sawtooth planar asperities for one or multiple distribution of angularity on the mean joint plane. There is major differences in behavior between this type of joint plane and irregular randomly distributed asperities on joint surfaces, with or without the presence of irregular structures, in relation with shear displacement and applied normal stress or load. One of these is the mobilized contact area and its evolution with shear area ratio (a_s), even if there is direct relationship between both ratio, the first being characterized by friction and sheared area of contact before peak shear strength but both ratio are identical after peak.

The principal difference in contact area between sawtooth planar asperities and irregular asperities joint plane types is that in the first case there is full contact after normal loading and phase I of friction mobilization with shear loading, while in the second case the proportion of contact areas on the samples surfaces is quite small in regards with the total area after normal loading (Gentier/1986). In this second case, friction linear mobilization of phase I increase the contact area, as stated earlier, while mobilization of dilatancy in phase II will reduce the contact area till reaching the peak shear strength, corresponding to around 0.55 mm of shear displacement where the contact area proportion remains extremely low, between 2.0 and 3.0% for three σ_N values tested: 7, 14 and 21 MPa (Fig. 6). In addition to roughness, the progressive degradation of the asperities and the evolution of contact (or sheared) areas were studied (Fig. 6) and are discused in detail in Riss et al. (this symposium). Paradoxically, it is shown that at peak shear strength the contact or sheared area is extremely low and seems the same for the three normal stress tested as if normal stress had no influence in this range.

It is shown (Fig. 6) that almost the totality of asperity degradation resulting in sheared area occurs between peak and a 3 mm of shear displacement corresponding to the progressive softening phase IV. Also, it is clearly demonstrated that asperity degradation depends not only on the magnitude or normal stress but mainly on shear displacement. Thus, at peak shear strength, the normal stress on contact areas is much higher than the mean applied normal stress, but despite this fact for the three relatively low normal stresses very few asperities were sheared off at peak strength. If the contact area is equal to the sheared area than for $\sigma_N = 7$ MPa and a contact area of 3% it means a contact normal stress of around 250 MPa which is three times σ_c. A more appropriate value related to σ_c means a contact area around 8.5% so the difference must be in friction giving no damaged area at failure. Nevertheless, it may be assumed that for low σ_N to values as high as $0.3\ \sigma_c$, most of the resisting shear force comes from friction on the sliding areas and from the work done by dilatancy against normal stress. But for higher σ_N values ($\sigma_N > 0.5\ \sigma_c$) an increasing proportion of asperities must failed with increasing sheared areas and a failure component must be part of a shear-dilatancy model.

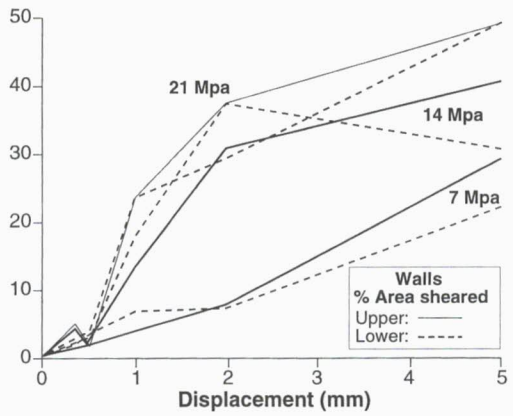

Figure 6. Proportion of damaged area evaluated on upper and lower joint walls for σn = 7, 14, 21 MPa in relation with shear displacement.

5 CONCLUSION

In the modelling approach, the 3D colatitudes (θ_3) must be used to characterize roughness angularities on the iregular joint surface instead of the usual 2D characterization. It must also integrate these characteristics in modelling peak shear srength taking into account simultaneous sliding on mobilized asperities

angularity and failure for higher asperity angularities. The shear behavior modelling must also integrate the degradation process on the joint wall surfaces as a function of the normal stress magnitude and shear displacement. Equally, these relationships must deal with the fundamental shear process on irregular joint surfaces, in which contact areas on the surface are limited and dependent on the normal stress magnitude in the pre-peak loading phase where the stresses are highly concentrated on these reduced areas. In the post-peak degradation phase of the joint surfaces the contact surface increases progressively as to release the stresses concentration, to reach finally a large surface of contact in the residual strength phase, as a function of shear displacement, where degradation is still operating on the joint shear plane to produce gouge material.

ACKNOWLEDGEMENT

This is a BRGM contribution n° 94059; this work was financially supported by a BRGM research project, an NSERC of Canada research grant and an NSERC graduate student followship.

REFERENCES

Archambault, G.,Gentier, S., Riss, J., Flamand, R. & Sirieix, C. 1995. A reevaluation of irregular joint shear behavior on the basis of 3D modelling of their morphology. Part II: Joint shear behavior mechanical modelling. *Proc.Mechanics of Jointed and Faulted Rock (MJFR-2)*: 163-168. Rotterdam: Balkema.

Bandis, S.C., Lumsden, A.C. & Barton, N.R. 1981. Fundamentals of rock joint deformation. *Int. J. Rock Mech. Sci. & Geomech.* Abstr. 13: 255-279.

Barton, N. 1973. Review of a new shear-strength criterion for rock joints. *Eng. Geol.* 7: 287-332.

Barton, N. & Stephansson, O. (Eds.) 1990. Rock Joints. *Proc. International Symposium on Rock Joints*, Loen, Norway, June 4-6.

Flamand, R., Archambault, G., Gentier, S., Riss, J. & Rouleau, A. 1994. An experimental study of the shear behavior of irregular joints based on angularies and progressive degradation of the surfaces. *Proc. 47th Canadian Geotechnical Conference of the C.G.S.*, Halifax, Nova Scotia, 253-262.

Gentier, S. 1986. Morphologie et comportement hydromécanique d'une fracture naturelle dans le granite sous contrainte normale; étude expérimentale et théorique. Documents du BRGM n° 134, BRGM, Orléans, France, 597 p.

Gentier, S. & Riss, J. 1990. Quantitative description and modelling of joints morphology. *Rock Joints:* 375-382. Barton & Stephansson (eds). Rotterdam: Balkema.

Gerrard, C. 1986. Shear failure of rock joints: appropriate constraints for empirical relations. *Int. J. Rock Mech. Min. Sci. & Geomech.* Abstr. 23, 6: 421-429.

Goodman, R.E. 1976. *Methods of Geological Engineering.* West Publishing Co. 472 p.

Goodman, R.E. & Myer, L. (Eds.) 1992. Fractured and Jointed Rock Masses. *Conference of ISRM Commission on Rock Joints*, Lake Tahoe, CA, June 3-5.

Haberfield, C.M. & Johnston, I.W. 1994. A mechanistically-based model for rough rock joints. *Int. J. Rock Mech. Min. Sci. & Geomech.* Abstr. 31, 4: 279-292.

Ladanyi, B. & Archambault, G. 1969. Simulation of shear behavior of a jointed rock mass. Rock mechanics - Theory and practice, *Proc. 11th Symp. on Roch Mech.,* California: 105-125.

Patton, F.D. 1966. Multiple modes of shear failure in rock. *Proc. 1st Congress ISRM,* Lisbon: 583-590.

Riss, J. & Gentier, S. 1989. Linear and areal roughness of non planar rock surfaces of fracture. *Acta Steorol* 8: 677-682.

Riss, J. & Gentier, S. 1990. Angularity of a natural fracture. *Proc. Int. Conf. on Mech. of Jointed and Faulted Rock,* Rossmanith P. (Ed.), Balkema, pp. 399-406.

Riss, J., Gentier, S., Archambault, G., Flamand, R. & Sirieix, C. 1995. A reevaluation of irregular joint shear behavior on the basis of 3D modelling of their morphology. Part I: Morphology description and 3D modelling. *Mechanics of Jointed and Faulted Rock (MJFR-2) Proc.*, Balkema, pp. 157-163.

Saeb, S. & Amadei, B. 1992. Modelling rock joints under shear and normal loading. *Int. J. Rock Mech. Sci. & Geomech.* Abstr. 29, 3: 267-278.

Scholtz, C.H. 1990. *The mechanics of eartquakes and faulting.* Cambridge University Press, 439 p.

Stephansson, O. (Ed.) 1985. Fundamentals of Rock Joints. *Proc. of the International Symposium on Fundamentals of Rock Joints,* Björkliden, Sweden, September 15-20.

Stephansson, O. & Jing, L. 1995. Testing and modeling of rock joints. *Proc. Mechanics of Jointed and Faulted*, Rossmanith (Ed.), Balkema, pp. 37-47.

Swan, G. & Zongqi, S. 1985. Prediction of shear behavior of joints using profiles. *Rock Mechanics and Rock Enginering* 18: 183-212.

Tabor, D. 1959. Junction growth in metallic friction. *Proc. Roy. Soc.* A. 251, 378.

Tse R. & Cruden, D.M. 1979. Estimating joint roughness coefficients. *Int. J. Rock Mech. Min. Sci. & Geomech.* Abstr. 16: 303-307.